FISEVIER

Contents lists available at ScienceDirect

# **Mathematical Biosciences**

journal homepage: www.elsevier.com/locate/mbs



Original Research Article

# Modeling the impact of non-human host predation on the transmission of Chagas disease

Xuan Dai <sup>a</sup>, Xiaotian Wu <sup>a,\*</sup>, Jiao Jiang <sup>a</sup>, Libin Rong <sup>b</sup>

- <sup>a</sup> School of Science, Shanghai Maritime University, Shanghai, 201306, PR China
- <sup>b</sup> Department of Mathematics, University of Florida, Gainesville, FL 32611, USA

# ARTICLE INFO

Keywords: Chagas disease Biting and defecation process Predation transmission Global stability

# ABSTRACT

In addition to the traditional transmission route via the biting-and-defecating process, non-human host predation of triatomines is recognized as another significant avenue for Chagas disease transmission. In this paper, we develop an eco-epidemiological model to investigate the impact of predation on the disease's spread. Two critical thresholds,  $\mathcal{R}^p_v$  (the basic reproduction number of triatomines) and  $\mathcal{R}^p_o$  (the basic reproduction number of the Chagas parasite), are derived to delineate the model's dynamics. Through the construction of appropriate Lyapunov functions and the application of the Bendixson–Dulac theorem, the global asymptotic stabilities of the equilibria are fully established. The vector-free equilibrium  $E_0$  is globally stable when  $\mathcal{R}^p_v < 1$ .  $E_1$ , the disease-free equilibrium, is globally stable when  $\mathcal{R}^p_v > 1$  and  $\mathcal{R}^p_0 < 1$ , while the endemic equilibrium  $E^*$  is globally stable when both  $\mathcal{R}^p_v > 1$  and  $\mathcal{R}^p_0 > 1$ . Numerical simulations highlight that the degree of host predation on triatomines, influenced by non-human hosts activities, can variably increase or decrease the Chagas disease transmission risk. Specifically, low or high levels of host predation can reduce  $\mathcal{R}^p_0$  to below unity, while intermediate levels may increase the infected host populations, albeit with a reduction in  $\mathcal{R}^p_0$ . These findings highlight the role played by non-human hosts and offer crucial insights for the prevention and control of Chagas disease.

# 1. Introduction

Chagas disease, also known as *American trypanosomiasis*, is a parasitic, systemic, and chronic illness that can infect both humans and other mammals. It is caused by the flagellate protozoan parasite *Trypanosoma cruzi (T. cruzi)* [1–3]. Globally, approximately 6 to 7 million people are infected with *T. cruzi*, and about 30 thousand new cases are identified annually across all forms of transmission. Furthermore, more than 75 million individuals are at risk of contracting the disease, primarily in 21 endemic countries in the Americas [1].

The *T. cruzi* parasite is typically transmitted to its reservoir hosts through contact with blood-sucking bugs of the subfamily Triatominae, commonly known as "kissing bugs". In certain regions, species like *Triatoma infestans* in Argentina and *Rhodnius prolixus* in Colombia are the primary vectors responsible for transmitting Chagas disease [1,4]. When these infected triatomine bugs bite humans, typically at exposed skin areas during the night, they deposit feces or urine near the bite wound. The parasites then enter the human hematological system through the host's scratching near the bites or through any skin lesions. Conversely, triatomine bugs acquire the parasites directly when they

feed on the blood of infected hosts, with the parasites entering their body systems through their salivary glands [1–3].

Many efforts are made to prevent and control Chagas disease, such as insecticide control campaigns [5,6] and the redevelopment of drugs targeting the chagas-parasite [7]. Despite significant progress in reducing the transmission of human T. cruzi infection in endemic areas, elimination remains elusive [1,8]. The complexity of T. cruzi involving interactions among humans, numerous wild/domestic animals, and diverse triatomine species, is the reason behind this [8,9]. Triatomine bugs infect not only humans but also various wild mammals like rodents and marsupials, as well as domesticated animals such as dogs and cats. Many sylvatic T. cruzi hosts, e.g., raccoons and opossums, omnivorous animals, exhibit considerably varying diets encompassing plants and small animals, including triatomine insects [10,11]. Surprisingly, armadillos almost exclusively consume triatomine insects [11]. Thus, triatomine insects constitute a significant portion of the diets of Chagas's parasite hosts, beyond their usual dietary intake. This highlights an important means of Chagas disease transmission known as predation transmission. Namely, the T. cruzi parasite can be transmitted to susceptible hosts when they prey on infected triatomine insects [10,

E-mail addresses: xtwu@shmtu.edu.cn (X. Wu), libinrong@ufl.edu (L. Rong).

<sup>\*</sup> Corresponding author.

11]. The evidence supporting this phenomenon is not uncommon in the existing literature. Several experimental studies have demonstrated that mammalian hosts can contract infections upon ingesting infected triatomine bugs [9,12]. From a molecular perspective, it has been elucidated that the critical factor underlying this phenomenon is attributed to a key molecule, gp82 [13]. Furthermore, recent research has confirmed that T. cruzi-infected insects induce higher rates of predation from intermediate hosts, with 36% of infected insects being preyed upon compared to 19% of uninfected ones, thereby promoting parasite transmission [14]. Hence, the vector consumption by hosts for parasite transmission may be an efficient pathway for Chagas-parasite transmission, potentially more effective than the traditional systemic transmission through insect biting and defecation [10,11]. Understanding this host-parasite-vector interaction, particularly the prey-predator mechanism, is crucial for comprehending the transmission of Chagas disease, not just academically but also for public health implications.

The majority of research efforts have been directed towards evaluating and controlling the transmission of the T. cruzi parasite from various perspectives. Some studies have concentrated on vector control strategies, such as insecticide spraying and housing improvements, aimed at eliminating domestic triatomine populations [15-18]. Other authors have focused on understanding parasite transmission and disease control by considering diverse parasite transmission routes and various stages of infection within the human population, aiming to comprehend the interaction between humans and triatomine insects [19-21]. Additionally, certain models have been employed to explore alternative modes of T. cruzi transmission and to examine contact process saturation, including Holling type I/II functional response models [11, 22]. Furthermore, diverse modeling approaches have been utilized to gain insights into the biology and ecology of T. cruzi transmission. Ordinary/delay differential equation systems have been formulated to identify thresholds determining the persistence and extinction of the disease or triatomine population [23-26]. Metapopulation models and reaction-diffusion equations have been applied to study the spatial distribution and invasion patterns of triatominae or T. cruzi populations [27–30]. Stochastic agent-based simulation models have also been developed to quantify and estimate the contact rate between hosts and vectors, the prevalence of the T. cruzi parasite in both hosts and vectors, and the abundance of host and vector populations [31,32].

Despite numerous studies aimed at understanding the biology, ecology, and epidemiology of Chagas disease transmission and the significant success achieved, the disease has re-emerged in endemic countries and is increasingly spreading to others [1]. The transmission cycle involving domestic and non-domestic animal hosts may potentially sustain the persistence of Chagas disease, posing a significant challenge to its long-term control. Yet, there remains a dearth of knowledge regarding the dynamic kinetics of *T. cruzi* transmission between animal hosts and triatomine vectors, particularly concerning the impact of predation transmission on the spread of the Chagas parasite. This gap in understanding prompts our objective in this study: to investigate how host predation transmission influences the dissemination of the Chagas parasite *T. cruzi* by formulating a mathematical model in the simplest manner possible.

The remainder of the paper is organized as follows: Section 2 outlines the formulation of the mathematical model based on the biological background of Chagas disease and the underlying hypothesis guiding our model construction. In Section 3, we theoretically explore the threshold dynamics, deriving the basic reproductive numbers of vector and parasite populations. Section 4 presents simulation results aimed at examining the impact of host predation transmission on the transmission of *T. cruzi*. Finally, a brief discussion and conclusion concludes the paper.

#### 2. Model formulation

Generally, once non-human hosts and triatomine vectors acquire the T. cruzi infection, they remain infectious for their lifetimes. Furthermore, infected triatomines and most non-human hosts are not pathogenic and do not exhibit any symptoms of Chagas disease [4]. Consequently, our model does not include recovery or disease-induced mortality for these populations. Additionally, the incubation periods of T. cruzi parasites within the bodies of triatomines and vertebrate hosts generally span 1–4 weeks and 3–7 days, respectively [33,34]. Given their long lifespans, and to capture the fundamental aspects of Chagas disease transmission in a simplified manner, we categorize both triatomine bugs and animal populations into susceptible  $(S_j)$  and infected  $(I_j)$  classes, where the subscript j=v,h denotes vector and host species, respectively. This categorization is consistent with previous studies [11,19,22].

Let  $r_v$  and  $\mu_v$  represent the natural birth and death rates per triatomine bug, respectively, where  $r_v > \mu_v$ . The carrying capacity of the triatomine population due to environmental constraints is represented by K. We assume that the total triatomine bug population  $(N_v(t))$  follows logistic growth in the absence of host predation and Chagas disease transmission. Consequently, the change in the total triatomine bug population is expressed by

$$N_v'(t) = (r_v - \mu_v)N_v \left(1 - \frac{N_v}{K}\right) = r_v N_v - \frac{r_v - \mu_v}{K}N_v^2 - \mu_v N_v,$$
 (1)

where the second term of the above equation indicates the density-dependent death of the triatomine population. Hence, in considering the susceptible and infected triatomine subpopulations, they are expected to satisfy the following set of differential equations

$$\begin{cases} S'_{v}(t) = r_{v} N_{v}(t) - \frac{r_{v} - \mu_{v}}{K} N_{v}(t) S_{v}(t) - \mu_{v} S_{v}(t), \\ I'_{v}(t) = -\frac{r_{v} - \mu_{v}}{K} N_{v}(t) I_{v}(t) - \mu_{v} I_{v}(t), \end{cases}$$
(2)

where both the susceptible and infected triatomine subpopulations have density-dependent mortality rates, and their offsprings are inherently susceptible, aligning with the biological aspects of Chagas disease.

Now, we define the change in the vector population considering systemic disease transmission through triatomine bugs' biting. Let a represent the biting rate per insect per unit of time, and b denote the transmission probability from infected hosts to susceptible vectors per bite. Consequently, the average infection rate of the susceptible triatomine bug subpopulation is given by the expression  $ba \frac{I_h(t)}{N_h(t)} S_v(t)$ , where  $N_h(t) = S_h(t) + I_h(t)$  represents the total number of the host population at time t. Subsequently, the system (2) can be expressed as follows

$$\begin{cases} S'_{v}(t) = r_{v}N_{v}(t) - ba\frac{I_{h}(t)}{N_{h}(t)}S_{v}(t) - \frac{r_{v} - \mu_{v}}{K}N_{v}(t)S_{v}(t) - \mu_{v}S_{v}(t), \\ I'_{v}(t) = ba\frac{I_{h}(t)}{N_{h}(t)}S_{v}(t) - \frac{r_{v} - \mu_{v}}{K}N_{v}(t)I_{v}(t) - \mu_{v}I_{v}(t). \end{cases}$$
(3)

As mentioned in the introduction, considering the presence of host predation transmission, both susceptible and infected triatomine bug subpopulations will diminish due to host predation at rates represented by  $f_p(N_v)N_h(t)\frac{S_v(t)}{N_v(t)}$  and  $f_p(N_v)N_h(t)\frac{I_v(t)}{N_v(t)}$ , respectively, where  $f_p(N_v)$  describes the functional response of host predation. Susceptible hosts may become infected when preying on infected insects at a rate denoted by  $pf_p(N_v)S_h(t)\frac{I_v(t)}{N_v(t)}$ , where p denotes the transmission probability of susceptible hosts per predation event. Additionally, the number of the host population will increase due to host predation on insects at a rate of  $\eta f_p(N_v)N_h(t)$ . All increases are assumed to be in the susceptible category, and  $\eta$  represents the efficiency with which predators convert consumed prey into new predators. For simplicity, we assume that hosts prey on insects following a linear functional response, expressed as

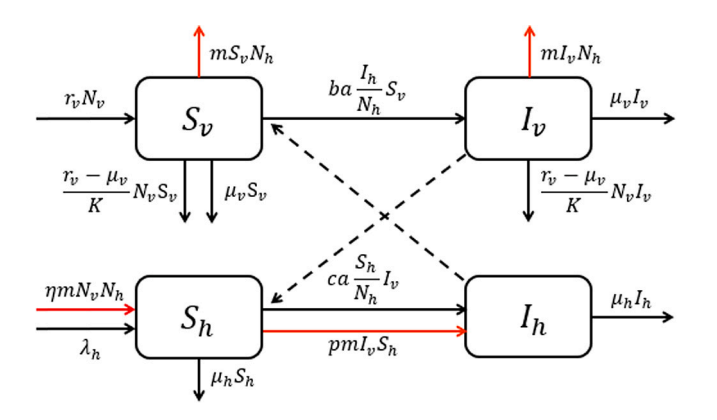


Fig. 1. The flowchart for model (4) encompasses systemic and predation transmission routes, portraying both triatomines and host populations through an SI model. Susceptible hosts are susceptible to infection via both systemic and predation transmissions, while susceptible vectors can solely acquire infection through systemic transmission when biting occurs.

 $f_p(N_v) = mN_v$ , where m denotes the per capita predation consumption rate

Consequently, by integrating the modified logistic growth rate of susceptible insects with the coexistence of both biting-defecation and predation transmissions, we can describe the interaction between triatomine bugs and host (animal) populations as follows

$$\begin{cases} S'_v(t) = r_v N_v(t) - ba \frac{I_h(t)}{N_h(t)} S_v(t) - m S_v(t) N_h(t) \\ - \frac{r_v - \mu_v}{K} N_v(t) S_v(t) - \mu_v S_v(t), \\ I'_v(t) = ba \frac{I_h(t)}{N_h(t)} S_v(t) - m I_v(t) N_h(t) - \frac{r_v - \mu_v}{K} N_v(t) I_v(t) - \mu_v I_v(t), \\ S'_h(t) = \lambda_h + \eta m (S_v(t) + I_v(t)) N_h(t) - p m I_v(t) S_h(t) \\ - ca \frac{S_h(t)}{N_h(t)} I_v(t) - \mu_h S_h(t), \\ I'_h(t) = p m I_v(t) S_h(t) + ca \frac{S_h(t)}{N_h(t)} I_v(t) - \mu_h I_h(t), \end{cases}$$

$$(4)$$

where  $\lambda_h$  denotes the rate of increase in susceptible host (animal) population, while c represents the transmission probability from infected triatomine to susceptible hosts per bite. Additionally,  $\mu_h$  stands for the natural death rate of the host population. We would like to emphasize that  $N_v(t) = S_v(t) + I_v(t)$  and  $N_h(t) = S_h(t) + I_h(t)$  denote the total numbers of vector and host populations, respectively. All model parameters are nonnegative, reflecting their biological implications.

The schematic diagram of model (4) is shown in Fig. 1, and Table 1 includes the description and the ranges of model parameter values.

# Proposition 1. Let

$$\begin{split} \mathcal{D} &= \left\{ (S_v, I_v, S_h, I_h) \in \mathbb{R}_+^4 \, : \, \eta(S_v + I_v) \right. \\ &+ \left. S_h + I_h \leq \frac{\eta K r_v^2 + 4 \lambda_h (r_v - \mu_v)}{4 (r_v - \mu_v) \min \left\{ \mu_v, \mu_h \right\}} \right\}, \end{split}$$

then the set  $\mathcal{D}$  is positively invariant for system (4). Moreover, the solution of this system is unique, nonnegative, and bounded for all time  $t \geq 0$  with the initial condition  $(S_n(0), I_n(0), S_h(0), I_h(0)) \in \mathcal{D}$ .

**Proof.** The vector field generated by the right sides of system (4) is Lipschitz continuous in  $\mathcal{D}$ . Thus, there exists a unique solution for all  $t \ge 0$ . The non-negativity of the solution of system (4), for all  $t \ge 0$  with the initial condition in  $\mathcal{D}$ , directly follows from Theorem 5.2.1 in [35].

Considering

$$\begin{split} &\eta N_v'(t) + N_h'(t) \\ &= \eta \cdot \left[ (r_v - \mu_v) N_v(t) (1 - \frac{N_v(t)}{K}) - m N_v(t) N_h(t) \right] \\ &+ \lambda_h + \eta m N_v(t) N_h(t) - \mu_h N_h(t) \\ &= \eta r_v N_v(t) - \eta \frac{r_v - \mu_v}{K} N_v^2(t) + \lambda_h - \eta \mu_v N_v(t) - \mu_h N_h(t) \\ &= \eta r_v N_v(t) \left[ 1 - \frac{N_v}{\widetilde{K}} \right] + \lambda_h - \eta \mu_v N_v(t) - \mu_h N_h(t) \\ &\leq \frac{\widetilde{K}}{4} \eta r_v + \lambda_h - \eta \mu_v N_v(t) - \mu_h N_h(t), \end{split}$$

where  $\widetilde{K}=\frac{r_v}{r_v-\mu_v}K$  and using the fact  $f(x)=x(1-\frac{x}{\widetilde{K}})\leq \frac{1}{4}\widetilde{K}$  for all  $x\geq 0$  and  $\widetilde{K}>0$ . We thus have

$$\frac{d}{dt}(\eta N_v(t) + N_h(t)) \le \left(\frac{\eta K}{4} \frac{r_v^2}{r_v - \mu_v} + \lambda_h\right) - \min\left\{\mu_v, \mu_h\right\} (\eta N_v(t) + N_h(t)),$$

which yields

$$\eta N_v(t) + N_h(t) \leq \frac{\eta K r_v^2 + 4\lambda_h(r_v - \mu_v)}{4(r_v - \mu_v) \min\left\{\mu_v, \mu_h\right\}} + (\eta N_v(0) + N_h(0)) \cdot e^{-\min\left\{\mu_v, \mu_h\right\}t}.$$

Therefore, we obtain

$$\lim \sup_{t \to +\infty} (\eta N_v(t) + N_h(t)) \leq \frac{\eta K r_v^2 + 4\lambda_h(r_v - \mu_v)}{4(r_v - \mu_v) \min\left\{\mu_v, \mu_h\right\}},$$

which implies that the set  $\mathcal{D}$  is positively invariant for system (4). Therefore, the boundedness of both insect vectors and host population sizes is guaranteed.  $\square$ 

#### 3. Global threshold dynamics of system (4)

It is evident that system (4) always exhibits an insect-free equilibrium  $E_0=(0,0,N_h^0,0)$ , where  $N_h^0=\lambda_h/\mu_h$ . Additionally, the system (4) yields a disease-free equilibrium  $E_1=(N_v^*,0,N_h^*,0)$  as well as an endemic equilibrium  $E^*=(S_v^*,I_v^*,S_h^*,I_h^*)$ . However, directly characterizing the global dynamics of this 4-D system is not straightforward. Therefore, our approach involves studying the dynamics of the total host and insect populations first.

# 3.1. Dynamics of total host and insect populations of system (4)

Adding the respective changes of total vector and host populations, model (4) reduces to the following 2-D system:

$$\begin{cases} N'_{v}(t) = r_{v}N_{v} - \frac{r_{v} - \mu_{v}}{K}N_{v}^{2}(t) - mN_{h}(t)N_{v}(t) - \mu_{v}N_{v}, \\ N'_{h}(t) = \lambda_{h} + \eta mN_{h}(t)N_{v}(t) - \mu_{h}N_{h}(t), \end{cases}$$
(5)

with initial values lying in  $\mathcal{D}_t = \{(N_v,N_h) \in \mathbb{R}^2_+ : \eta N_v + N_h \leq \frac{\eta K r_v^2 + 4\lambda_h(r_v - \mu_v)}{4(r_v - \mu_v) \min[\mu_v, \mu_h]} \}$ . It is clear that the above planar system has an insect-free equilibrium  $E_0^t = (0,N_h^0)$ . Following the next generation matrix method and notations in [39,40], the new birth matrix and the transfer matrix of the triatomine bugs at  $E_0^t$  are

$$F=r_v, \quad V=mN_h^0+\mu_v,$$

respectively. Therefore, the basic reproduction number of the triatomine population of model (5) is the spectral radius of  $FV^{-1}$ , given by

$$\mathcal{R}_{v}^{p} = \rho(FV^{-1}) = \frac{r_{v}}{mN_{b}^{0} + \mu_{v}}.$$
(6)

This threshold represents the number of offspring produced by a susceptible triatomine bug throughout its entire lifespan in the absence of disease infection. It essentially determines whether the triatomine population will persist or become extinct in the long term.

Table 1

Parameter description and ranges.

Parameter	Description	Range/value	Reference
$r_v$	Natural birth rate per triatomine bug	[0.0786, 1.071]/day	[19,36]
K	Carrying capacity of triatomine population	[3000,30000]	[22]
a	Number of bites per bug per unit time	[0.2, 33]/day	[37]
5	Transmission probability per $I_v$ bite on a $S_h$	[0.00026,0.06]	[25,38]
2	Transmission probability per $S_v$ bite on an $I_h$	[0.005,0.49]	[25,38]
D	Transmission probability from $I_v$ to $S_h$ during host predation	[0.108,0.177]	[22]
m	Predation rate per prey per predator	varied	assumed
7	Trophic conversion efficiency	varied	assumed
$\lambda_h$	Recruitment rate of susceptible hosts (e.g. raccoon) per unit time	[0.00247,0.01288]/day	[22]
$\mu_h$	Natural death rate per host (e.g. raccoon)	[0.00109,0.00274]/day	[22]
$\mu_v$	Natural death rate per triatomine bug	[0.0045,0.0083]/day	[25,38]

**Lemma 2.** For the host-vector interaction model (5),  $E_0^t$  is globally asymptotically stable in  $D_t$  if  $\mathcal{R}_v^p < 1$  and unstable if  $\mathcal{R}_v^p > 1$ .

**Proof.** The local stability and instability of  $E_0^t$  immediately follows from Theorem 2 in [40]. Next, we show the global asymptotic stability of the equilibrium when  $\mathcal{R}_p^p < 1$ .

For the total host population, we have

$$N_h'(t) = \lambda_h + \eta m N_h(t) N_v(t) - \mu_h N_h(t) \geq \lambda_h - \mu_h N_h(t).$$

By the comparison principle [41], we have

$$N_h(t) \ge N_h(0)e^{-\mu_h t} + \lambda_h \int_0^t e^{-\mu_h(t-s)} ds = N_h(0)e^{-\mu_h t} + N_h^0(1 - e^{-\mu_h t}),$$

implying

 $\lim_{t \to \infty} \inf N_h(t) \ge N_h^0.$ 

For the total vector population, we have

$$N'_{v}(t) \le (r_{v} - \mu_{v})N_{v}(t) - mN_{h}^{0}N_{v}(t) = (\mu_{v} + mN_{h}^{0})(\mathcal{R}_{v}^{p} - 1)N_{v}(t).$$

It follows from the comparison principle [41] again that

$$0 \le \lim_{t \to \infty} \sup N_v(t) \le \lim_{t \to \infty} N_v(0) e^{(\mu_v + mN_h^0)(\mathcal{R}_v^p - 1)t} = 0$$

when  $\mathcal{R}_{v}^{p} < 1$ . Hence, in the case of  $\mathcal{R}_{v}^{p} < 1$ , we have

$$\lim_{t\to\infty} N_v(t) = 0, \quad \text{for any } N_v(0) \ge 0.$$

Thus, for the limiting system of the original system (5), the host population reduces to

$$N_h'(t) = \lambda_h - \mu_h N_h(t), \tag{7}$$

which yields

$$\lim_{t \to \infty} N_h(t) = N_h^0, \quad \text{for any } N_h(0) \ge 0.$$

Accordingly,  $E_0^t = (0, N_h^0)$  of system (5) is globally asymptotically stable in  $\mathcal{D}_t$  if  $\mathcal{R}_v^p < 1$ .  $\square$ 

**Lemma 3.** For the host–vector interaction model (5), there admits a unique coexistent equilibrium  $E_1^t = (N_v^*, N_h^*)$ , which is globally asymptotically stable in  $D_t$  if and only if  $\mathcal{R}_v^p > 1$ .

**Proof.** Let  $E_1^t = (N_v^*, N_h^*)$  be the coexistent positive equilibrium of model (5). Setting the right sides of system (5) to zeros results in

$$\begin{cases} (r_{v} - \mu_{v})N_{v}^{*} \left(1 - \frac{N_{v}^{*}}{K}\right) - mN_{h}^{*}N_{v}^{*} = 0, \\ \lambda_{h} + \eta mN_{h}^{*}N_{v}^{*} - \mu_{h}N_{h}^{*} = 0. \end{cases}$$
(8)

From the second equation of Eq. (8), we can solve  $N_h^*$  as

$$N_h^* = \frac{\lambda_h}{\mu_h - \eta m N_v^*} > 0 \Leftrightarrow N_v^* < \frac{\mu_h}{\eta m}.$$
 (9)

Substituting Eq. (9) into the first equation of Eq. (8) yields the following quadratic equation of  $N_{\cdot}^{*}$ 

$$\left(N_{v}^{*}\right)^{2} - \left(K + \frac{\mu_{h}}{\eta m}\right)N_{v}^{*} + \frac{\mu_{h}K\left(\mu_{v} + mN_{h}^{0}\right)}{\eta m(r_{v} - \mu_{v})}\left(\mathcal{R}_{v}^{p} - 1\right) = 0.$$
 (10)

In terms of biological rationale and straightforward algebraic calculations based on Eq. (10), we ascertain that system (5) exhibits a unique coexistent equilibrium  $E_1^l = (N_v^l, N_h^s)$  if and only if  $\mathcal{R}_v^p > 1$ , where

$$0 < N_v^* = \frac{1}{2} \left[ \left( K + \frac{\mu_h}{\eta m} \right) - \sqrt{\Delta} \right] < \frac{\mu_h}{\eta m}, \quad N_h^* = \frac{2\lambda_h/(\eta m)}{(\frac{\mu_h}{\eta m} - K) + \sqrt{\Delta}} > N_h^0,$$
(11)

and

$$\Delta = \left(K - \frac{\mu_h}{\eta m}\right)^2 + 4 \frac{K \lambda_h}{\eta (r_v - \mu_v)} > 0.$$

We will show  $E_1^t$  is globally asymptotically stable in  $\mathcal{D}_t$  if  $\mathcal{R}_v^p>1$ . Let us construct the Lyapunov function

$$L_1\left(N_v(t),N_h(t)\right) = \eta\left(N_v-N_v^*-N_v^*\ln\frac{N_v}{N_v^*}\right) + \left(N_h-N_h^*-N_h^*\ln\frac{N_h}{N_h^*}\right).$$

Differentiating  $L_1$  along the solutions of (5) gives

$$\begin{split} \frac{\mathrm{d}L_1}{\mathrm{d}t} &= \eta \left( 1 - \frac{N_v^*}{N_v} \right) \frac{\mathrm{d}N_v}{\mathrm{d}t} + \left( 1 - \frac{N_h^*}{N_h} \right) \frac{\mathrm{d}N_h}{\mathrm{d}t} \\ &= \eta (N_v - N_v^*) \left[ (r_v - \mu_v)(1 - \frac{N_v}{K}) - mN_h \right] \\ &+ (N_h - N_h^*) \left[ \frac{\lambda_h}{N_h} + \eta mN_v - \mu_h \right] \\ &= \eta (N_v - N_v^*) \left[ \frac{(r_v - \mu_v)}{K} N_v^* - \frac{(r_v - \mu_v)}{K} N_v + mN_h^* - mN_h \right] \\ &+ (N_h - N_h^*) \left[ \frac{\lambda_h}{N_h} + \eta mN_v - \frac{\lambda_h}{N_h^*} - \eta mN_v^* \right] \\ &= -\frac{\eta (r_v - \mu_v)}{K} (N_v - N_v^*)^2 - \frac{\lambda_h}{N_h N_h^*} (N_h - N_h^*)^2 \\ &< 0 \end{split}$$

It is clear that the above equality holds if and only if  $(N_v(t), N_h(t)) = (N_v^*, N_h^*)$ . By LaSalle's Invariance Principle [42],  $E_1^t = (N_v^*, N_h^*)$  is globally asymptotically stable with respect to  $\mathcal{D}_t$  if  $\mathcal{R}_v^p > 1$ .  $\square$ 

According to Eq. (6), there exists a critical value for the host predation rate, denoted as  $m_1^* = \frac{r_v - \mu_v}{N_h^0}$ , such that  $\mathcal{R}_v^p(m_1^*) = 1$ . At this critical

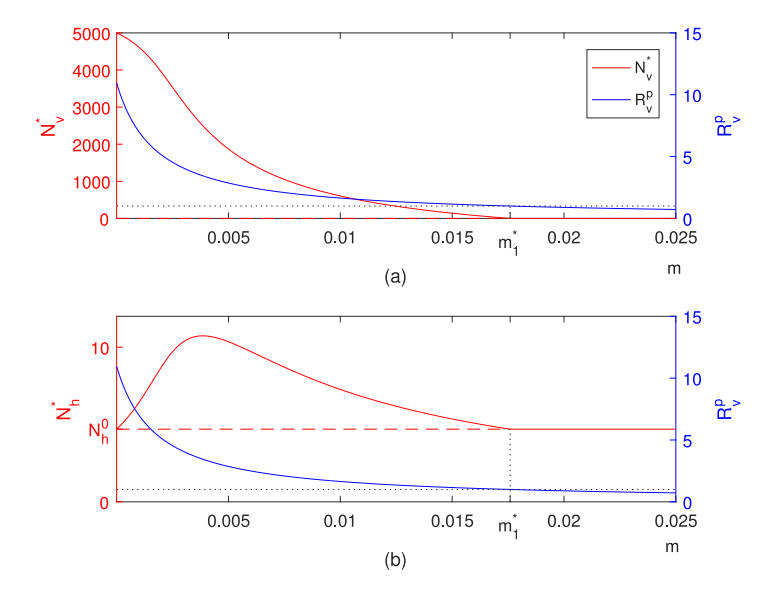


**Fig. 2.** Bifurcation diagram of model (5) in terms of the predation rate m. The other parameters are  $r_v = 0.091$ , K = 5000, a = 0.2, b = 0.00026, c = 0.005, p = 0.177,  $\eta = 0.00016$ ,  $\mu_h = 0.00274$ ,  $\lambda_h = 0.01288$ ,  $\mu_v = 0.0083$ , and  $m_1^* = 0.0176$ .

threshold, the equilibrium  $E_1^t$  is globally stable if  $m < m_1^*$ , whereas  $E_0^t$  is globally stable if  $m > m_1^*$ . This result essentially implies that a high host predation rate reduces the risk of Chagas disease transmission. Fig. 2 shows the bifurcation diagram of model (5) in terms of the parameter m. It is clear that a high predation rate m leads to the extinction of the triatomine population, thereby eliminating the risk of Chagas disease.

**Theorem 4.** The insect-free equilibrium  $E_0 = (0, 0, N_h^0, 0)$  of system (4) is globally asymptotically stable in D when  $\mathcal{R}_v^p < 1$  and unstable when  $\mathcal{R}_v^p > 1$ .

**Proof.** The results in [43,44] claim that the behavior of the resulting limiting system asymptotically approaches that of the original system at equilibrium. This conclusion directly follows from Lemmas 2 and 3. From a biological standpoint, this indicates that the triatomine bug population goes extinct if and only if  $\mathcal{R}_p^p < 1$ .

## 3.2. Dynamics of infected host and insect populations

In the following, we assume  $\mathcal{R}_{v}^{p} > 1$ . According to the results in [43, 44], the long-term dynamics of system (4) asymptotically approaches its limiting system. As per Lemma 3, when  $\mathcal{R}_{v}^{p} > 1$ , system (4) reduces to the following limiting system:

$$\begin{cases} S'_{v}(t) = \hat{r}_{v} - \hat{\beta}_{v} S_{v}(t) I_{h}(t) - (mN_{h}^{*} + \hat{\mu}_{v}) S_{v}(t), \\ I'_{v}(t) = \hat{\beta}_{v} S_{v}(t) I_{h}(t) - (mN_{h}^{*} + \hat{\mu}_{v}) I_{v}(t), \\ S'_{h}(t) = \hat{\lambda}_{h} - (pm + \hat{\beta}_{h}) I_{v}(t) S_{h}(t) - \mu_{h} S_{h}(t), \\ I'_{h}(t) = (pm + \hat{\beta}_{h}) I_{v}(t) S_{h}(t) - \mu_{h} I_{h}(t), \end{cases}$$

$$(12)$$

where

$$\hat{r}_{v} = r_{v} N_{v}^{*}, \ \hat{\mu}_{v} = \mu_{v} + \frac{r_{v} - \mu_{v}}{K} N_{v}^{*}, 
\hat{\lambda}_{h} = \lambda_{h} + \eta m N_{v}^{*} N_{h}^{*} > 0, \ \hat{\beta}_{v} = \frac{ba}{N^{*}}, \ \hat{\beta}_{h} = \frac{ca}{N^{*}}.$$
(13)

System (12) can further reduce to the planar system

$$\begin{cases} I'_{v}(t) = \widehat{\beta}_{v}(N_{v}^{*} - I_{v}(t))I_{h}(t) - (mN_{h}^{*} + \widehat{\mu}_{v})I_{v}(t), \\ I'_{h}(t) = (pm + \widehat{\beta}_{h})I_{v}(t)(N_{h}^{*} - I_{h}(t)) - \mu_{h}I_{h}(t), \end{cases}$$
(14)

with the initial condition lying in the invariant set  $\mathcal{D}_d = \{(I_v, I_h) \in \mathcal{R}^2_+: 0 \leq I_v \leq N_v^*, 0 \leq I_h \leq N_h^*\}.$ 

The above planar system has a disease-free equilibrium  $\hat{E}_0 = (I_v, I_h) = (0, 0)$ . Following the next generation matrix method [39,40], we can define the new infection matrix as

$$F = \begin{pmatrix} 0 & \widehat{\beta}_v N_v^* \\ (pm + \widehat{\beta}_h) N_h^* & 0 \end{pmatrix},$$

and the transfer matrix as

$$V = \begin{pmatrix} mN_h^* + \widehat{\mu}_v & 0 \\ 0 & \mu_h \end{pmatrix}.$$

Subsequently, the basic reproduction number of model (12) (also of the Chagas disease model (4)) is

$$\mathcal{R}_{0}^{p} = \rho(FV^{-1}) = \sqrt{\frac{\hat{\beta}_{v} N_{v}^{*}}{m N_{h}^{*} + \hat{\mu}_{v}} \frac{(pm + \hat{\beta}_{h}) N_{h}^{*}}{\mu_{h}}},$$
(15)

where  $N_v^*$  and  $N_h^*$  are determined by Eqs. (11), respectively.

It follows from Theorem 2 in [40] that  $\hat{E}_0$  is locally asymptotically stable if  $\mathcal{R}_0^p < 1$  and unstable if  $\mathcal{R}_0^p > 1$  with respect to  $\mathcal{D}_d$ .

**Lemma 5.** For the limiting system (14), the disease-free equilibrium  $\hat{E}_0$  is globally asymptotically stable in  $\mathcal{D}_d$  when  $\mathcal{R}_0^p < 1$ .

**Proof.** In case of  $\mathcal{R}_0^p < 1$ , we consider the following Lyapunov function

$$L_2(I_v(t), I_h(t)) = (pm + \hat{\beta}_h)N_h^* \cdot I_v(t) + (mN_h^* + \hat{\mu}_v) \cdot I_h(t).$$

Differentiating  $L_2$  along the solution of system (14) yields

$$\begin{split} \frac{\mathrm{d}L_2}{\mathrm{d}t} &= (pm + \widehat{\beta}_h)N_h^* \frac{\mathrm{d}I_v(t)}{\mathrm{d}t} + (mN_h^* + \widehat{\mu}_v) \frac{\mathrm{d}I_h(t)}{\mathrm{d}t} \\ &= (pm + \widehat{\beta}_h)N_h^* \left[ \widehat{\beta}_v(N_v^* - I_v)I_h - (mN_h^* + \widehat{\mu}_v)I_v \right] \\ &+ (mN_h^* + \widehat{\mu}_v) \left[ (pm + \widehat{\beta}_h)I_v(N_h^* - I_h) - \mu_h I_h \right] \\ &= \left[ \widehat{\beta}_v N_v^* (pm + \widehat{\beta}_h)N_h^* - (mN_h^* + \widehat{\mu}_v)\mu_h \right] I_h \\ &- \left[ \widehat{\beta}_v (pm + \widehat{\beta}_h)N_h^* + (mN_h^* + \widehat{\mu}_v)(pm + \widehat{\beta}_h) \right] I_h I_v \\ &= \mu_h (mN_h^* + \widehat{\mu}_v)((\mathcal{R}_p^0)^2 - 1) \left( 1 - \psi I_v \right) I_h, \end{split}$$

where

$$\psi = \frac{\widehat{\beta_v}(pm + \widehat{\beta_h})N_h^* + (mN_h^* + \widehat{\mu_v})(pm + \widehat{\beta_h})}{\widehat{\beta_v}N_v^*(pm + \widehat{\beta_h})N_h^* - (mN_h^* + \widehat{\mu_v})\mu_h}$$

$$=\frac{\widehat{\beta}_v(pm+\widehat{\beta}_h)N_h^*+(mN_h^*+\widehat{\mu}_v)(pm+\widehat{\beta}_h)}{(mN_h^*+\widehat{\mu}_v)\mu_h((R_0^n)^2-1)}\leq 0.$$

Hence, we obtain  $\frac{dL_2}{dt} \leq 0$  if  $\mathcal{R}_0^p < 1$ . Moreover,

$$\frac{\mathrm{d}L_{2}\left(I_{v}(t),I_{h}(t)\right)}{\mathrm{d}t}=0$$

if and only if  $(I_v(t), I_h(t)) = (0,0) = \hat{E}_0$ . By LaSalle's Invariance Principle [42],  $\hat{E}_0$  is globally asymptotically stable with respect to  $\mathcal{D}_d$ when  $\mathcal{R}_0^p < 1$ .  $\square$ 

**Theorem 6.** System (4) admits a unique disease-free equilibrium  $E_1$  =  $(N_n^*, 0, N_h^*, 0)$ , which is globally asymptotically stable in  $\mathcal{D}$  when  $\mathcal{R}_n^p > 1$ and  $\mathcal{R}_0^p < 1$ .

**Proof.** The proof follows directly from Lemmas 3 and 5. It indicates that the triatomine bug population persists, while Chagas disease dies out when  $\mathcal{R}_{v}^{p} > 1$  and  $\mathcal{R}_{0}^{p} < 1$ .  $\square$ 

Lemma 7. For the limiting system (14), there admits a unique endemic equilibrium  $\hat{E}_1 = (I_v^*, I_h^*)$  if  $\mathcal{R}_0^p > 1$ , and it is globally asymptotically stable

**Proof.** In case of  $\mathcal{R}_0^p > 1$ , letting the right hands of system (14) be

$$\begin{cases} \hat{\beta}_{v}(N_{v}^{*} - I_{v}^{*})I_{h}^{*} - (mN_{h}^{*} + \hat{\mu}_{v})I_{v}^{*} = 0, \\ (pm + \hat{\beta}_{h})I_{v}^{*}(N_{h}^{*} - I_{h}^{*}) - \mu_{h}I_{h}^{*} = 0. \end{cases}$$
(16)

A straightforward algebraical calculation of Eqs. (16) leads to

$$I_{v}^{*} = \frac{(mN_{h}^{*} + \widehat{\mu}_{v})\mu_{h}}{(pm + \widehat{\beta}_{h})(mN_{h}^{*} + \widehat{\mu}_{v} + \widehat{\beta}_{v}N_{h}^{*})} \left( (\mathcal{R}_{0}^{p})^{2} - 1 \right) > 0, \tag{17}$$

$$I_h^* = \frac{mN_h^* + \hat{\mu}_v}{\hat{\beta}_v} \frac{I_v^*}{N_v^* - I_v^*} > 0.$$
 (18)

This implies the occurrence of a unique endemic equilibrium  $\hat{E}_1$  =  $(I_n^*, I_h^*)$  for the limiting system (14).

The Jacobian matrix at  $\hat{E}_1$ 

$$J(\widehat{E}_1) = \begin{pmatrix} -\left(\widehat{\beta}_v I_h^* + mN_h^* + \widehat{\mu}_v\right) & \widehat{\beta}_v S_v^* \\ (pm + \widehat{\beta}_h) S_h^* & -\left((pm + \widehat{\beta}_h) I_v^* + \mu_h\right) \end{pmatrix} \triangleq \begin{pmatrix} -a_1 & b_1 \\ b_2 & -a_2 \end{pmatrix}$$

The corresponding characteristic equation is

$$\lambda^2 + (a_1 + a_2)\lambda + a_1 a_2 - b_1 b_2 = 0. {19}$$

$$\Delta = (a_1 + a_2)^2 - 4(a_1a_2 - b_1b_2) = (a_1 - a_2)^2 + 4b_1b_2 > 0.$$

Moreover, we have  $\lambda_1 + \lambda_2 = -(a_1 + a_2) < 0$  and

$$\begin{split} \lambda_1 \cdot \lambda_2 &= a_1 a_2 - b_1 b_2 \\ &= \left( \widehat{\beta}_v I_h^* + m N_h^* + \widehat{\mu}_v \right) \left( (p m + \widehat{\beta}_h) I_v^* + \mu_h \right) - \widehat{\beta}_v S_v^* (p m + \widehat{\beta}_h) S_h^* \\ &= \left( \widehat{\beta}_v I_h^* + m N_h^* + \widehat{\mu}_v \right) \left( (p m + \widehat{\beta}_h) I_v^* + \mu_h \right) \\ &\times \left( 1 - \frac{\widehat{\beta}_v S_v^*}{\widehat{\beta}_v I_h^* + (m N_h^* + \widehat{\mu}_v)} \frac{(p m + \widehat{\beta}_h) S_h^*}{(p m + \widehat{\beta}_h) I_v^* + \mu_h} \right) \\ &= \left( \widehat{\beta}_v I_h^* + m N_h^* + \widehat{\mu}_v \right) \left( (p m + \widehat{\beta}_h) I_v^* + \mu_h \right) \left( 1 - \frac{S_v^* S_h^*}{N_v^* N_v^*} \right) > 0, \end{split}$$

where the relationship at the equilibrium (Eqs. (16)) is used. Thus, the eigenvalues of the characteristic Eq. (19) are real and negative, which implies that  $\hat{E}_1$  is locally asymptotically stable in  $\mathcal{D}_d$  when  $\mathcal{R}_0^p > 1$ .

Next, we let

$$\begin{pmatrix} f(I_v,I_h) \\ g(I_v,I_h) \end{pmatrix} \triangleq \begin{pmatrix} \widehat{\beta}_v(N_v^*-I_v(t))I_h(t) - (mN_h^*+\widehat{\mu}_v)I_v(t) \\ (pm+\widehat{\beta}_h)I_v(t)(N_h^*-I_h(t)) - \mu_hI_h(t) \end{pmatrix}.$$

Constructing Dulac function  $B(I_v, I_h) = 1 \in \mathbb{C}^1(\mathcal{D}_d)$  yields

$$\begin{split} &\frac{\partial (B(I_v,I_h)f(I_v,I_h))}{\partial I_v} + \frac{\partial (B(I_v,I_h)g(I_v,I_h))}{\partial I_h} \\ &= - \hat{\beta}_v I_h - (mN_h^* + \hat{\mu}_v) - (pm + \hat{\beta}_h)I_v - \mu_h < 0, \quad \forall (I_v,I_h) \in \mathcal{D}_d. \end{split} \tag{20}$$

By the Bendixson-Dulac Theorem, there are no nonconstant periodic solutions lying entirely within the region  $D_d$ . Thus,  $\hat{E}_1$  is globally

asymptotically stable in  $\mathcal{D}_d$  when  $\mathcal{R}_0^p > 1$ .

Alternatively, because  $\frac{\partial f}{\partial I_h} = \beta_v(N_v^* - I_v(t)) \ge 0$  and  $\frac{\partial g}{\partial I_v} = (pm + \widehat{\beta}_h)(N_h^* - I_h(t)) \ge 0$ , system (14) is cooperative in the domain  $\mathcal{D}_d$ . Moreover, system (14) has a disease-free equilibrium  $\hat{E}_0=(0,0)$  and a unique endemic equilibrium  $\hat{E}_1=(I_v^*,I_h^*)$ . According to Theorem 3.2.2 in [35],  $\hat{E}_1$  is globally attractive, indicating that  $\hat{E}_1$  is globally asymptotically stable in  $\mathcal{D}_d$ .  $\square$ 

**Theorem 8.** System (4) admits a unique endemic equilibrium  $E^* =$  $(S_v^*, I_v^*, S_h^*, I_h^*)$  when  $\mathcal{R}_v^p > 1$  and  $\mathcal{R}_0^p > 1$ , where  $I_v^*$  and  $I_h^*$  are determined by Eqs. (17)–(18) and  $S_v^* + I_v^* = N_v^*, S_h^* + I_h^* = N_h^*$ . Moreover,  $E^*$  is globally asymptotically stable in  $\mathcal{D}$ .

The proof follows directly from Lemmas 3 and 7. Biologically, the Chagas disease is spreading when  $\mathcal{R}_{v}^{p} > 1$  and  $\mathcal{R}_{o}^{p} > 1$ .

## 3.3. Without predation transmission

Host predation suppresses the number of vector populations, thereby reducing the risk of Chagas disease transmission. Conversely, the total host population increases due to nutrient uptake from insect prey, consequently amplifying the risk. Therefore, studying how host predation on insects either amplifies or suppresses the risk of Chagas disease transmission is both necessary and meaningful.

In the absence of host predation on insects, i.e. m = 0, the model (4) becomes

The Jacobian matrix at 
$$\hat{E}_{1}$$
 is
$$J(\hat{E}_{1}) = \begin{pmatrix} -\left(\hat{\beta}_{v}I_{h}^{*} + mN_{h}^{*} + \hat{\mu}_{v}\right) & \hat{\beta}_{v}S_{v}^{*} \\ (pm + \hat{\beta}_{h})S_{h}^{*} & -\left((pm + \hat{\beta}_{h})I_{v}^{*} + \mu_{h}\right) \end{pmatrix} \triangleq \begin{pmatrix} -a_{1} & b_{1} \\ b_{2} & -a_{2} \end{pmatrix},$$
where  $S_{v}^{*} = N_{v}^{*} - I_{v}^{*}$  and  $S_{h}^{*} = N_{h}^{*} - I_{h}^{*}$ , and  $a_{1}, a_{2}, b_{1}, b_{2}$  are all positive.
$$S_{v}^{\prime}(t) = r_{v}N_{v}(t) - \hat{\beta}_{v}^{np}I_{h}(t)S_{v}(t) - \frac{r_{v} - \mu_{v}}{K}N_{v}(t)I_{v}(t) - \mu_{v}I_{v}(t),$$

$$S_{h}^{\prime}(t) = \hat{\beta}_{v}^{np}I_{h}(t)S_{v}(t) - \frac{r_{v} - \mu_{v}}{K}N_{v}(t)I_{v}(t) - \mu_{v}I_{v}(t),$$

$$S_{h}^{\prime}(t) = \hat{\beta}_{v}^{np}S_{h}(t)I_{v}(t) - \mu_{h}S_{h}(t),$$

$$I_{h}^{\prime}(t) = \hat{\beta}_{h}^{np}S_{h}(t)I_{v}(t) - \mu_{h}I_{h}(t),$$

$$I_{h}^{\prime}(t) = \hat{\beta}_{h}^{np}S_{h}(t)I_{v}(t) - \mu_{h}I_{h}(t),$$

$$(21)$$

where  $\beta_v^{np} = ba/N_h^0$ ,  $\beta_h^{np} = ca/N_h^0$  and  $N_h^0 = \lambda_h/\mu_h$ .

For system (21), it is evident that it allows for an insect-free equilibrium  $E_0^{np} = (0, 0, N_h^0, 0)$  and a disease-free equilibrium  $E_1^{np} = (S_v^0, 0, N_h^0, 0)$ , where  $S_v^0 = K$ . Utilizing the next generation matrix method outlined in [39,40], we can determine the basic reproduction numbers of the insect and parasite populations as follows

$$\mathcal{R}_{v}^{np} = \frac{r_{v}}{\mu_{v}} > \frac{r_{v}}{mN_{v}^{0} + \mu_{v}} = \mathcal{R}_{v}^{p} \tag{22}$$

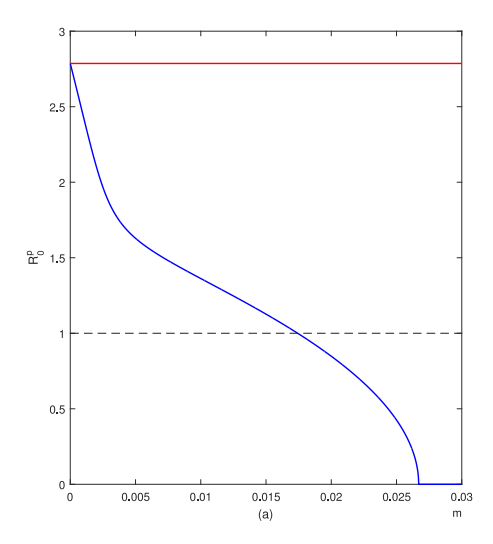
$$\mathcal{R}_{0}^{np} = \sqrt{\frac{\beta_{v}^{np} S_{v}^{0}}{\mu_{v} + \frac{r_{v} - \mu_{v}}{\kappa} S_{v}^{0}} \frac{\beta_{h}^{np} N_{h}^{0}}{\mu_{h}}},$$
(23)

respectively.

We summarize the dynamics of system (21) in terms of  $\mathcal{R}_{v}^{np}$  and  $\mathcal{R}_{0}^{np}$ 

Theorem 9. For system (21), we have

(i)  $E_0^{np}$  is always unstable since  $\mathcal{R}_v^{np} > 1$ .



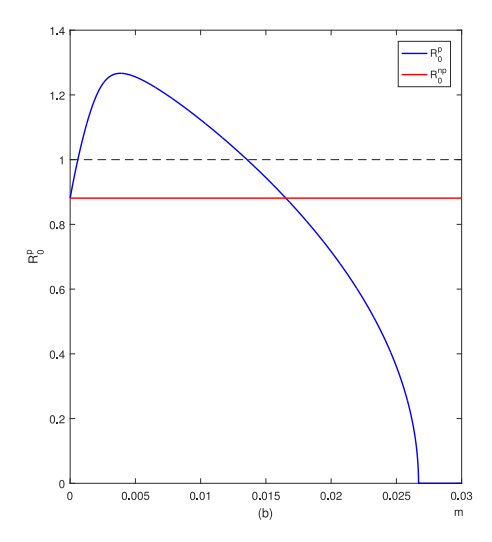


Fig. 3. The relationship between  $\mathcal{R}_0^n$  and m, and between  $\mathcal{R}_0^{np}$  and m, where parameter values are:  $\eta=0.00016,~\mu_h=0.00274,~\lambda_h=0.01288,~K=5000,~r_v=0.13,~\mu_v=0.0045,~p=0.177,~a=0.2,~b=0.0013,~and~c=0.05$  in the left panel while c=0.005 in the right panel.

(ii)  $E_1^{np}$  is globally asymptotically stable when  $\mathcal{R}_0^{np} < 1$ ; there is a unique endemic equilibrium  $E_2^{np} = (S_v^*, I_v^*, S_h^*, I_h^*)$  with  $S_v^* + I_v^* = S_v^0$  and  $S_h^* + I_h^* = N_h^0$ , which is globally asymptotically stable when  $\mathcal{R}_0^{np} > 1$ .

It is evident that  $\mathcal{R}^p_v$  is a monotonically decreasing function of the predation rate m, specifically  $\mathcal{R}^p_v < \mathcal{R}^{np}_v$ . Particularly, an increase in the predation rate m can alter  $\mathcal{R}^p_v$  from being above unity to below, ultimately resulting in the extinction of the triatomine population. However, the relationship between  $\mathcal{R}^p_0$  and m is more complex. As depicted in Fig. 3, with an increase in the predation rate m,  $\mathcal{R}^p_0$  can either monotonically decrease until reaching zero or initially increase, reach a peak value, and then decline to zero. In the former scenario, we consistently observe  $\mathcal{R}^p_0 < \mathcal{R}^{np}_0$ , suggesting that the predation rate m reduces the risk of Chagas disease transmission. However, in the latter case, as m increases,  $\mathcal{R}^p_0$  surpasses  $\mathcal{R}^{np}_0$  to reach a peak, and then decreases again to fall below  $\mathcal{R}^{np}_0$ . Notably,  $\mathcal{R}^p_0$  can transition from being below unity to above, and vice versa, as m increases.

#### 4. Numerical results

In this section, we conduct numerical explorations to illustrate the dynamic behavior of system (4) and the impact of host predation on disease transmission. The parameter value ranges are detailed in Table 1. The simulations were executed using Matlab, version R2016a. Note that for the lower value of  $r_v$ , we estimated it as follows: considering the minimum number of fertile eggs (41) produced by R. colombensis during its life cycle of 357 days, along with the proportion of insects that complete their life cycle (68.5%) [36], the minimum daily birth rate is calculated using the formula  $41/357 \times 68.5\% = 0.0786$ .

#### 4.1. Simulation of asymptotic behaviors

Fig. 4 displays the solutions of system (4) when  $\mathcal{R}_v^P < 1$ . As anticipated, the counts of susceptible and infected vectors swiftly converge to zeros, while the counts of susceptible hosts converge to  $N_h^0$ , and the counts of infected hosts converge to zeros.

When  $\mathcal{R}_v^p > 1$  and  $\mathcal{R}_0^p < 1$ , the solution curves of system (4) are presented in Fig. 5. It is evident that all solutions converge to the disease-free equilibrium  $E_1 = (N_v^*, 0, N_h^*, 0)$ , signifying the eventual dissipation of Chagas disease. Additionally, oscillations are observed in Fig. 5 due to the presence of the predator–prey mechanism.

Similarly, the solution curves of system (4) when  $\mathcal{R}_v^p > 1$  and  $\mathcal{R}_0^p > 1$  are shown in Fig. 6. As shown in the analysis in the previous section, all solutions converge to a unique positive endemic equilibrium  $E^* = (S_v^*, I_v^*, S_h^*, I_h^*)$ .

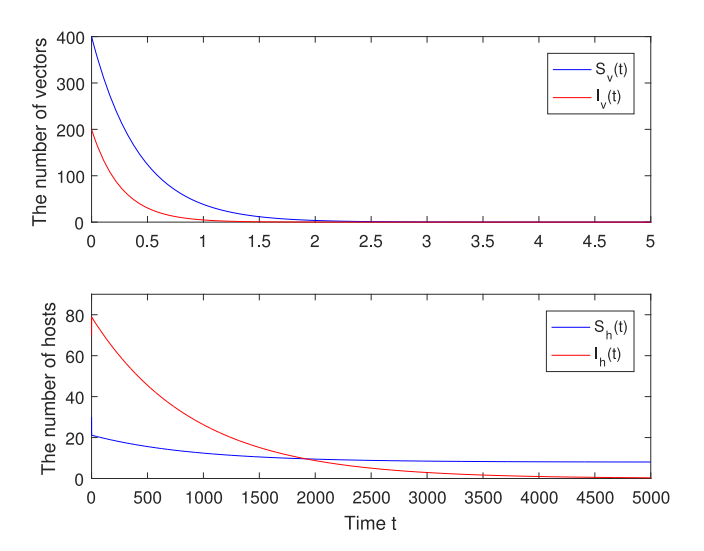


**Fig. 4.** Numerical solutions of system (4) converge in time to  $E_0=(0,0,N_h^0.0)$  if  $\mathcal{R}_v^p=0.6241<1$ . The parameter values are  $\eta=0.00016,\ m=0.025,\ \mu_h=0.0011,\ \lambda_h=0.0088,\ K=5000,\ r_p=0.13,\ \mu_v=0.0083,\ p=0.177,\ a=0.2,\ b=0.00026,\ c=0.005.$ 

# 4.2. Impact of predation transmission on the spread of Chagas disease

To explore the impact of host predation transmission on the spread of Chagas disease, we conducted simulations to understand the relationship between predation-related model parameters  $(m, \eta, \text{ and } p)$  and disease scale-related indices  $(\mathcal{R}_0^p, I_v^*, \text{ and } I_h^*)$ .

The impact of the predation rate m on the spread of Chagas disease is important. Fig. 7 illustrates the relationship among the counts of infected hosts  $I_h^*$ , infected vectors  $I_v^*$ , the basic reproduction number of the Chagas parasite  $\mathcal{R}_0^p$ , and the predation rate m. With an increase in m,  $\mathcal{R}_0^p$  initially rises from below unity to above, reaches a peak, and then declines to zero.

Moreover, two thresholds,  $m_2^*$  and  $m_3^*$ , exist. When  $m < m_2^*$  or  $m > m_3^*$ , both  $I_v^*$  and  $I_h^*$  are zeros; however, when m falls within the range  $(m_2^*, m_3^*)$ , they take positive values. This observation indicates that an intermediate level of host predation on insects leads to a Chagas disease outbreak, while the disease can diminish for low or high degrees of host predation. Note that the non-monotonicity of infected populations and  $\mathcal{R}_0^p$  with the predation rate m, as shown in Fig. 7, is preserved for high values of  $r_v$ .

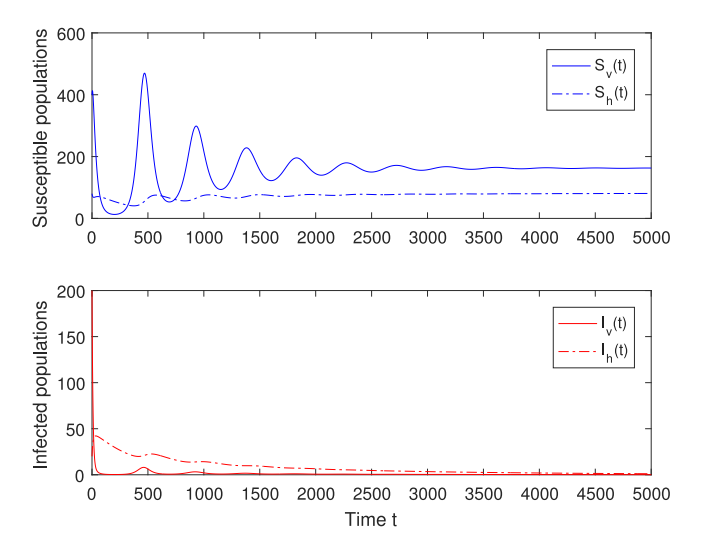


**Fig. 5.** Numerical solutions of system (4) converge in time to  $E_1=(N_v^*,0,N_h^*,0)$  when  $\mathcal{R}_v^p=12.2973>1$  and  $\mathcal{R}_0^p=0.9038<1$ . The parameters are  $\eta=0.015,\ m=0.001,\ \mu_h=0.00247,\ \lambda_h=0.00247,\ K=5000,\ r_v=0.091,\ \mu_v=0.0064,\ p=0.177,\ a=0.2,\ b=0.0271,\ c=0.01.$ 

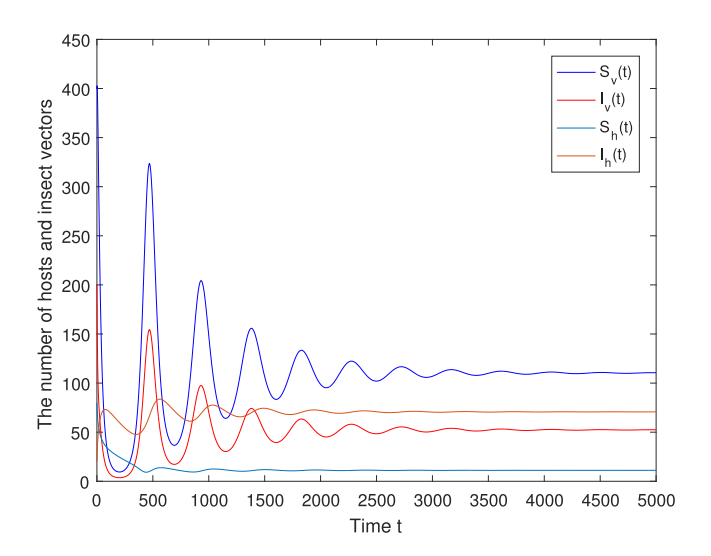


**Fig. 6.** Numerical solutions of system (4) converge in time to  $E_* = (S_v^*, I_v^*, S_h^*, I_h^*)$  when  $\mathcal{R}_v^p = 12.2973 > 1$  and  $\mathcal{R}_0^p = 3.4131 > 1$ . The parameters are  $\eta = 0.015$ , m = 0.001,  $\mu_h = 0.00247$ ,  $\lambda_h = 0.00247$ , K = 5000,  $r_v = 0.091$ ,  $\mu_v = 0.0064$ , p = 0.177, a = 1, b = 0.05, c = 0.01.

Besides the predation rate m, the impact of other predation-related parameters such as  $\eta$  and p on the transmission of Chagas disease is also significant. Figs. 8(a,b) illustrate that  $\mathcal{R}_0^p$  either monotonically decreases or increases with the rise of  $\eta$  or p, respectively. It can transition from being above unity to below, and vice versa.

Furthermore, Fig. 8(c) demonstrates that an increase in  $\eta$  consistently leads to a decrease in  $I_v^*$ , while  $I_h^*$  initially shows an increasing trend followed by a subsequent decline to a lower level. On the other hand, a higher infection probability p resulting from host predation on insects consistently yields larger numbers of both  $I_v^*$  and  $I_h^*$  (refer to Fig. 8(d)). Consequently, a high trophic conversion efficiency  $(\eta)$  coupled with a low infection probability p can cause  $\mathcal{R}_0^p$  to be less than 1, effectively controlling the spread of Chagas disease.

# 4.3. Sensitivity analysis on $\mathcal{R}_0^p$

To ascertain the relative significance of model parameters in Chagas disease transmission, a sensitivity analysis was conducted on the basic

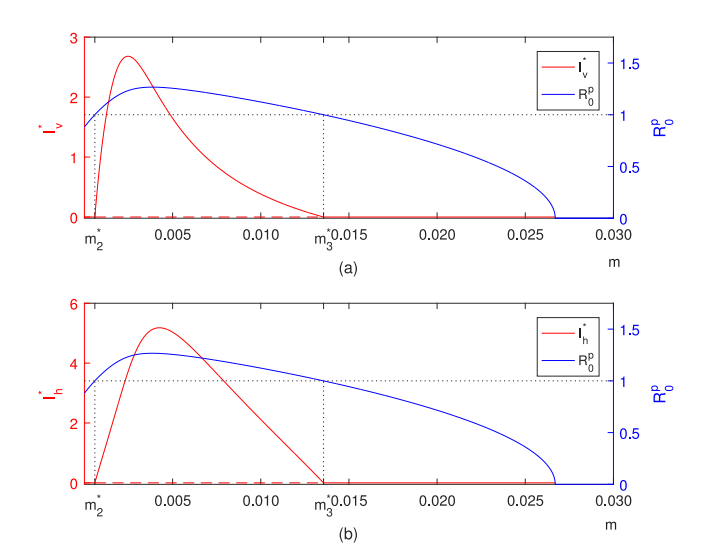


**Fig. 7.** Impact of the predation rate m on the numbers of infected hosts  $(I_h^*)$  and infected vectors  $(I_v^*)$ , as well as on  $\mathcal{R}_p^0$ . The parameter values are  $\eta=0.00016$ ,  $\mu_h=0.00274$ ,  $\lambda_h=0.01288$ , K=5000,  $r_v=0.13$ ,  $\mu_v=0.0045$ , p=0.177, a=0.2, b=0.0013, c=0.005, and  $m_2^*=0.00059$ ,  $m_3^*=0.0136$ .

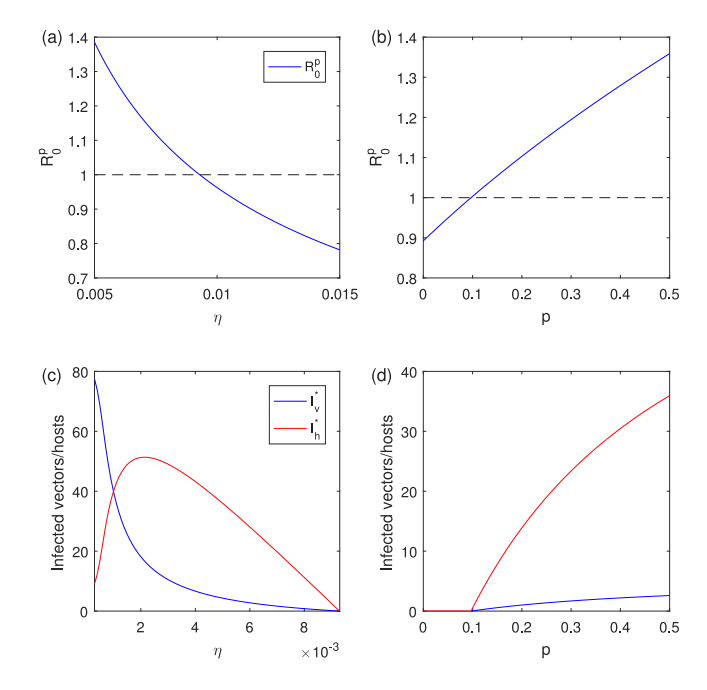


**Fig. 8.** The influence of trophic conversion efficiency  $(\eta)$  and the probability of predation-induced infection (p) on the numbers of infected hosts  $(I_h^*)$  and infected vectors  $(I_v^*)$ , as well as on  $\mathcal{R}_0^p$ . The other parameter values are  $\mu_h=0.00274,\ \lambda_h=0.01288,\ K=5000,\ r_v=0.091,\ \mu_v=0.0064,\ a=0.6,\ b=0.00271,\ c=0.05.$ 

reproduction number of the Chagas parasite  $\mathcal{R}^p_0$ , defined in Eq. (15). This analysis utilized the Latin hypercube sampling (LHS) method with 1000 samples and assessed the partial rank correlation coefficients (PRCCs) [45]. The baseline values of these parameters were set to the mean within the ranges specified in Table 1, using a uniform distribution for parameter allocation. As shown in Fig. 9, the birth rate of insect vectors  $(r_v)$ , trophic conversion efficiency  $(\eta)$ , insect biting rate (a), and transmission probabilities (b and c) exert significant influence on  $\mathcal{R}^p_0$ . The sensitivity of the host predation rate (m) is relatively moderate, while parameters such as K, p,  $\mu_v$ , and  $\mu_h$  show minor sensitivity.

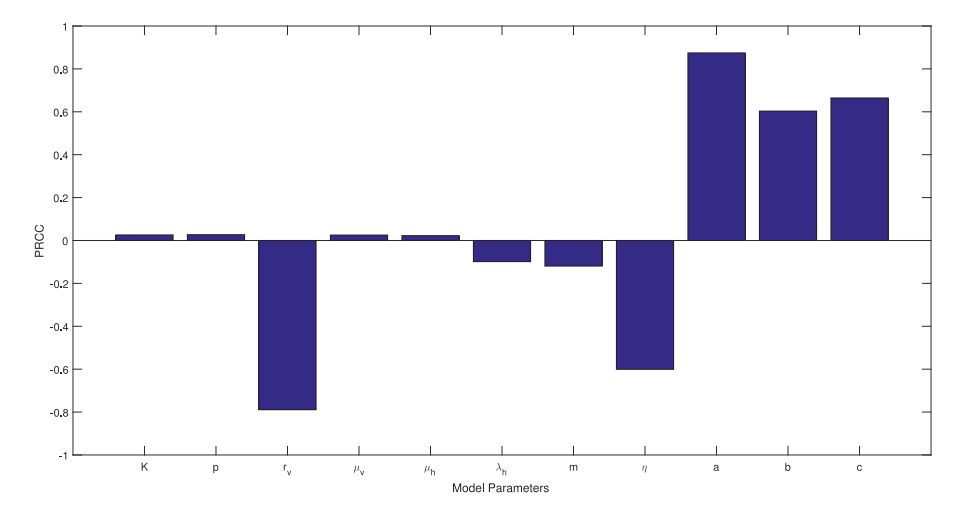


Fig. 9. The PRCC results for all model parameters regarding  $\mathcal{R}_0^p$  were obtained using 1000 samples. For the parameters K, p,  $\mu_v$ , and  $\mu_h$ , the p-values were found to be  $\leq$  0.05. The baseline values of these parameters are as follows:  $\eta=0.01$ , m=0.01, m=0.01

#### 5. Discussion and conclusion

In this study, we developed a mathematical model (4) to examine the potential impact of non-human host predation on insects regarding the transmission of Chagas disease. Besides the conventional systemic transmission usually attributed to blood-sucking triatomine bugs, we introduced an essential route of host predation transmission into the model. This additional transmission mode significantly influences the dynamics of both host and insect populations, thereby impacting the risk of Chagas disease transmission.

Using the basic reproduction numbers of insect and T. cruzi parasite  $(\mathcal{R}_v^p)$  and  $\mathcal{R}_0^p)$ , our study established conditions that determine the persistence or extinction of Chagas disease spread. These results might offer critical insights for the prevention and control of Chagas disease.

Due to the complexity of the 4-dimensional system, directly presenting the global dynamics of these equilibria can be challenging. Nonetheless, by studying two 2-D systems, constructing suitable Lyapunov functions, and employing the Bendixson-Dulac theorem, we successfully demonstrated the global asymptotic stabilities of the proposed 4-D model. Specifically, we initially investigated a 2-D system concerning total vector and host populations, showcasing the global stability of population dynamics in terms of  $\mathcal{R}_{v}^{p}$ . Subsequently, utilizing the longterm behavior of the resulting limiting system, which asymptotically mirrors the original system, we further explored another 2-D disease system. Corresponding global stabilities were investigated in terms of  $\mathcal{R}_0^p$  in combination with Lyapunov functions and the Bendixson–Dulac theorem. Consequently, we established that if  $\mathcal{R}_{v}^{p} < 1$ , the insect-free equilibrium  $E_0=(0,0,N_h^0,0)$  of system (4) is globally asymptotically stable. Similarly, if  $\mathcal{R}_v^p>1$  and  $\mathcal{R}_0^p<1$ , the disease-free equilibrium  $E_1 = (N_v^*, 0, N_h^*, 0)$  is globally asymptotically stable. If both  $\mathcal{R}_v^p > 1$ and  $\mathcal{R}_0^p > 1$ , the system (4) converges to an endemic equilibrium  $E^* =$  $(S_v^*, I_v^*, S_h^*, I_h^*)$ , which is globally asymptotically stable (see Theorems 4, 6, and 8).

Numerical simulations were conducted to explore the impact of non-human host predation on insects on the transmission of Chagas disease. The results indicated that in the presence of host predation on insects, both low and high host predation rates (m) can lead to the extinction of infected vector and host populations, thereby preventing the spread of Chagas disease. However, when m falls within an effective intermediate range, increasing m can either augment or diminish the numbers of infected vectors and hosts (refer to Fig. 7). The infection probability of predation transmission (p) notably escalates the risk of Chagas disease transmission (see Fig. 8(b,d)). Despite the decrease in  $\mathcal{R}_0^p$  due to the trophic conversion efficiency  $\eta$ , the number of  $I_b^*$  may

still increase (refer to Fig. 8(c)), indicating an elevated risk of Chagas disease transmission.

Sensitivity analysis revealed that, for those predation-related parameters to  $\mathcal{R}_{0}^{p}$ , trophic conversion efficiency  $(\eta)$  exhibits great sensitivity, and the predation rate (m) displays an intermediate sensitivity, whereas the sensitivity of the probability of predation transmission (p) is minor (refer to Fig. 9). These findings underscore the critical role played by non-human host predation transmission in the spread of Chagas disease, emphasizing the necessity for further experimental results to develop more effective biological interventions for its prevention and control.

With evidence of susceptible hosts acquiring infection through the consumption of infected vectors, Kribs-Zaleta et al. [11,22] previously developed models incorporating predation transmission to quantify parameter estimations for different contact process saturation levels during biting and predation. Their findings suggested that parasites can persist endemically even if the threshold of the vector basic reproduction number is less than unity, and a Holling-type II functional response for the predation term can lead to bi-stability of the Chagas parasite population. Our recent modeling study also revealed that the maximum predation rate of Holling-type II response plays a key role in giving rise to the bi-stability of Chagas disease [46]. Coffield et al. [21] developed a compartment simulation model considering the combination of vector, human, and animal populations involving biting, congenital, and predation/oral transmission routes. They concluded that the effect of predation transmission is complicated. As the consumption rate increases, the prevalence/number of infected humans can either initially increase up to a peak value and then decline, persistently increase, or directly decrease, while the prevalence/number of infected animals substantially increases. However, none of the previous studies include the trophic conversion of hosts due to the consumption of vectors, which is common biologically. To the best of our knowledge, the model proposed in the current study is the first one to integrate the full prey-predator mechanism. That is, the increase of hosts induced by host predation was newly considered in the model. As a result, we were able to show the specific thresholds for the extinction and endemicity of Chagas disease. Our numerical findings revealed that the high prevalence of Chagas infection as shown in Fig. 6 is possible, which confirms the field studies in [47,48], where up to 58% of infected vectors are attained in contiguous forests. Moreover, the nonmonotonicity of infected populations was observed in this study, which is also noticed by another study with predation transmission [21]. The very low level of prevalence of the infected population is possible due to the high predation rate in this study. The reason behind this may be attributed to the joint effect of multiple factors such as host predation and trophic conversion. As we can see from the model, a high predation rate leads to an increase in the numbers of both susceptible and infected hosts due to trophic conversion and predation infection, meanwhile it, in turn, reduces the number of vectors due to the consumption by hosts, hence eventually leading to extinction of parasites. Overall, our modeling study shows the fundamental role played by non-human primates in causing the complexity of Chagas disease transmission.

Despite the progress made in understanding the complexity of Chagas disease within the interactions of host-parasite-vector, our comprehension of Chagas disease transmission remains incomplete. In the future, this model could be enhanced by incorporating the phenomenon of behavioral changes in triatomine bugs when infected with the Chagas parasite [14]. Moreover, we recognize the current limitations in data availability for precise model calibration, the variability of parameter values in simulations derived from multiple sources, and without inclusion of disease-induced death, which could lead to a backward bifurcation phenomenon as demonstrated in the study [49]. Nonetheless, our theoretical modeling remains adaptable and scalable for future field investigations. Additionally, the current model relies on the simplest linear functional response of predation, whereas a saturable process in predation, such as the Holling type II response, might provide a more accurate approximation of the reality of Chagas disease transmission. The existence of various host categories (e.g., raccoons, armadillos, and humans, among others) might introduce different mechanisms affecting the complexity of Chagas disease transmission. These issues remain to be addressed in future investigations.

## CRediT authorship contribution statement

Xuan Dai: Writing – review & editing, Writing – original draft, Investigation, Formal analysis, Conceptualization. Xiaotian Wu: Writing – review & editing, Writing – original draft, Supervision, Investigation, Funding acquisition, Conceptualization. Jiao Jiang: Writing – review & editing, Writing – original draft, Investigation, Conceptualization. Libin Rong: Writing – review & editing, Writing – original draft, Supervision, Funding acquisition, Conceptualization.

# Declaration of competing interest

The article is original and the authors declare that they have no competing of interests.

### Data availability

No data was used for the research described in the article.

# Acknowledgments

X. Wu would like to thank the financial support from the National Natural Science Foundation of China (No. 12271346 and 12071300). L. Rong is supported by the National Science Foundation, United States grants DMS-1950254 and DMS-2324692. The authors thank three anonymous reviewers for their insightful comments which improved the manuscript.

# References

- World Health Organization, Chagas disease (also known as American trypanosomiasis), 2023, https://www.who.int/news-room/fact-sheets/detail/ chagas-disease-(american-trypanosomiasis), (Accessed 13 January 2023).
- [2] K.C.F. Lidani, F.A. Andrade, L. Bavia, F.S. Damasceno, M.H. Beltrame, I.J. Messias-Reason, T.L. Sandri, Chagas disease: from discovery to a worldwide health problem, Front. Public Health. 7 (2019) 166.
- [3] A. Requena-Méndez, E. Aldasoro, E. de Lazzari, E. Sicuri, M. Brown, D.A. Moore, J. Gascon, J. Muñoz, Prevalence of chagas disease in latin-American migrants living in Europe: a systematic review and meta-analysis, PLoS Negl. Trop. Dis. 9 (2015) e0003540.

- [4] A.B.B. de Oliveira, K.C.C. Alevi, C.H.L. Imperador, F.F. Madeira, M.T.V. Azeredo-Oliveira, Parasite-vector interaction of Chagas disease: A mini-review, Am. J. Trop. Med. Hyg. 98 (2018) 653–655.
- [5] G. Mougabure-Cueto, M.I. Picollo, Insecticide resistance in vector Chagas disease: evolution, mechanisms and management, Acta Trop, 149 (2015) 70–85.
- [6] L.I. Rodríguez-Planes, M.S. Gaspe, G.F. Enriquez, R.E. Gürtler, Impacts of residual insecticide spraying on the abundance and habitat occupancy of Triatoma sordida and co-occurrence with Triatoma infestans: A three-year follow-up in northeastern Argentina, Acta Tropica. 202 (2020) 105251.
- [7] P. García-Huertas, N. Cardona-Castro, Advances in the treatment of Chagas disease: Promising new drugs, plants and targets, Biomed. Pharmacother. 142 (2021) 112020.
- [8] R.E. Gürtler, M.C. Cecere, G.M. Vázquez-Prokopec, L.A. Ceballos, J.M. Gurevitz, M.d.P. Fernández, et al., Domestic animal hosts strongly influence human-feeding rates of the Chagas disease vector Triatoma infestans in Argentina, PLoS Negl. Trop. Dis. 8 (5) (2014) e2894.
- [9] A.M. Jansen, S.C.D.C. Xavier, A.L.R. Roque, Landmarks of the knowledge and Trypanosoma cruzi biology in the wild environment, Front. Cell. Infect. Microbiol. 10 (2020) 10.
- [10] D. Erazo, J. Cordovez, C. Cabrera, J.E. Calzada, A. Saldaña, N.L. Gottdenker, Modelling the influence of host community composition in a sylvatic Trypanosoma cruzi system, Parasitology 144 (2017) 1881–1889.
- [11] C. Kribs-Zeleta, Vector consumption and contact process saturation in sylvatic transmission of *Tcruzi*, Math. Popul. Stud. 13 (2006) 135–152.
- [12] F.L. Rocha, A.L. Roque, J.S. de Lima, C.C. Cheida, F.G. Lemos, F.C. de Azevedo, et al., Trypanosoma cruzi infection in neotropical wild carnivores (Mammalia: Carnivora): at the top of the T. cruzi transmission chain, PLoS One 8 (7) (2013) 673662.
- [13] N. Yoshida, Molecular mechanisms of trypanosoma cruzi infection by oral route, Mem. Inst. Oswaldo Cruz. 104 (2009) 101–107.
- [14] N.P. Marliére, M.G. Lorenzo, A.A. Guarneri, Trypanosoma cruzi-infected Rhodnius prolixus endure increased predation facilitating parasite transmission to mammal hosts, PLoS Negl. Trop. Dis. 15 (7) (2021) e0009570.
- [15] A.M. Spagnuolo, M. Shillor, L. Kingsland, A. Thatcher, M. Toeniskoetter, B. Wood, A logistic delay differential equation model for chagas disease with interrupted spraying schedules, J. Biol. Dyn. 6 (2012) 377–394.
- [16] B. Oduro, M.J. Grijalva, W. Just, A model of insect control with imperfect treatment, J. Biol. Dyn. 13 (2019) 518–537.
- [17] C.Y. Han, H. Issa, J. Rychtář, D. Taylor, N. Umana, A voluntary use of insecticide treated nets can stop the vector transmission of Chagas disease, PLoS Negl. Trop. Dis. 14 (2020) e0008833.
- [18] C. Nieto-Sanchez, B.R. Bates, D. Guerrero, S. Jimenez, E.G. Baus, K. Peeters Grietens, M.J. Grijalva, Home improvement and system-based health promotion for sustainable prevention of Chagas disease: A qualitative study, PLoS Negl. Trop. Dis. 13 (2019) e0007472.
- [19] B.Y. Lee, S.M. Bartsch, L. Skrip, D.L. Hertenstein, C.M. Avelis, M. Ndeffo-Mbah, et al., Are the London Declaration's 2020 goals sufficient to control Chagas disease?: Modeling scenarios for the Yucatan Peninsula, PLoS Negl. Trop. Dis. 12 (2018) 1–20
- [20] H. Inaba, H. Sekine, A mathematical model for Chagas disease with infection-age-dependent infectivity, Math. Biosci. 190 (2004) 39–69.
- [21] D.J. Coffield, A.M. Spagnuolo, M. Shillor, E. Mema, B. Pell, A. Pruzinsky, et al., A model for Chagas disease with oral and congenital transmission, PLoS One 8 (6) (2013) e67267.
- [22] C. Kribs-Zaleta, Estimating contact process saturation in sylvatic transmission of Trypanosoma cruzi in the United States, PLoS Negl. Trop. Dis. 4 (2010) e656.
- [23] X. Wu, D. Gao, Z. Song, J. Wu, Modelling triatomine bug population and Trypanosoma rangeli transmission dynamics: Co-feeding, pathogenic effect and linkage with chagas disease, Math. Biosci. 324 (2020) 108326.
- [24] X. Wu, D. Gao, Z. Song, J. Wu, Modelling Trypanosoma cruzi-Trypanosoma rangeli co-infection and pathogenic effect on Chagas disease spread, Discrete Cont. Dyn-B. 28 (2023) 1024–1045.
- [25] M.A. Acuña-Zegarra, D. Olmos-Liceaga, J.X. Velasco-Hernández, The role of animal grazing in the spread of Chagas disease, J. Theoret. Biol. 457 (2018) 19–28
- [26] D.J. Coffield, A.M. Spagnuolo, Steady state stability analysis of a chagas disease model, BIOMATH 3 (1) (2014) 1405261.
- [27] L.I. Rodríguez-Planes, M.S. Gaspe, G.F. Enriquez, R.E. Gürtler, Habitat-specific occupancy and a metapopulation model of Triatoma sordida (Hemiptera: Reduviidae), a secondary vector of Chagas Disease, in Northeastern Argentina, J. Med. Entomol. 55 (2018) 370–381.
- [28] B. Crawford, C. Kribs-Zaleta, A metapopulation model for sylvatic T. cruzi transmission with vector migration, Math. Biosci. Eng. 11 (2014) 471–509.
- [29] V. Steindorf, N.A. Maidana, Modeling the spatial spread of chagas disease, Bull. Math. Biol. 81 (2019) 1687–1730.
- [30] D.J. Coffield, A.M. Spagnuolo, R. Capouellez, G.A. Stryker, A mathematical model for Chagas disease transmission with neighboring villages, Front. Appl. Math. Stat. 9 (2023) 1225137.
- [31] K.E. Yong, A. Mubayi, C.M. Kribs, Agent-based mathematical modeling as a tool for estimating Trypanosoma cruzi vector-host contact rates, Acta Trop, 151 (2015) 21–31.

- [32] N. Saadi, A. Bah, T. Mahdjoub, C. Kribs-Zaleta, On the sylvatic transmission of T. cruzi, the parasite causing Chagas disease: A view from an agent-based model, Ecol. Model. 423 (2020) 109001.
- [33] A. Kollien, G. Schaub, The development of Trypanosoma cruzi in triatominae, Parasitol, Today 16 (2000) 381–387.
- [34] L.M. de Pablos Torrò, L. Retana Moreira, A. Osuna, Extracellular vesicles in Chagas disease: A new passenger for an old disease, Front. Microbiol. 9 (2018) 1190
- [35] H.L. Smith, Monotone Dynamical Systems: An Introduction To the Theory of Competitive and Cooperative Systems, American Mathematical Society, 1995.
- [36] A. Arèvalo, J.C. Carranza, F. Guhl, J.A. Clavijo, G.A. Vallejo, Comparison of the life cycles of Rhodnius colombiensis Moreno, Jurberg and Galvão, 1999 and R. prolixus Stal, 1872 (Hemiptera, Reduviidae, Triatominae) under laboratory conditions, Biomedica: revista del Instituto Nacional de Salud 27 (2007) 119–129.
- [37] J.E. Rabinovich, J.A. Leal, D.F. de Pinero, Domiciliary biting frequency and blood ingestion of the chagasis disease vector Rhodnius prolixus stahl (hemiptera: reduviidae) in Venezuela, Trans. R. Soc. Trop. Med. Hyg. 73 (1979) 272–283.
- [38] N. Tomasini, P.G. Ragone, S. Gourbière, J.P. Aparicio, P. Diosque, Epidemiological modeling of Trypanosoma cruzi: Low stercorarian transmission and failure of host adaptive immunity explain the frequency of mixed infections in humans, PLoS Comput. Biol. 13 (2017) e1005532.
- [39] O. Diekmann, J.A. Heesterbeek, J.A. Metz, On the definition and the computation of the basic reproduction ratio  $R_0$  in models for infectious diseases in heterogeneous populations, J. Math. Biol. 28 (1990) 365–382.
- [40] P. van den Driessche, J. Watmough, Reproduction numbers and sub-threshold endemic equilibria for compartmental models of disease transmission, Math. Biosci. 180 (2002) 29–48.

- [41] H.L. Smith, P. Waltman, The Theory of the Chemostat, Cambridge University Press. 1995.
- [42] N.F. Britton, Essential Mathemmatical Biology, Springer, London, 2005.
- [43] H.R. Thieme, Convergence results and a Poincaré-Bendixson trichotomy for asymptotically autonomous differential equations, J. Math. Biol. 30 (1992) 755-763.
- [44] H.R. Thieme, Asymptotically autonomous differential equations in the plane, Rocky Mountain J. Math. 24 (1994) 351–380.
- [45] S. Marino, I.B. Hogue, C.J. Ray, D.E. Kirschner, A methodology for performing global uncertainty and sensitivity analysis in systems biology, J. Theoret. Biol. 254 (2008) 178–196.
- [46] J. Jiang, D. Gao, J. Jiang, X. Wu, Assessing the impact of host predation with Holling II response on the transmission of Chagas disease, Math. Appl. Sci. Eng. 13 (2) (2023) 623–643.
- [47] S.F. Brenière, S. Pietrokovsky, E.M. Gastélum, M.F. Bosseno, M.M. Soto, A. Ouaissi, et al., Feeding patterns of Triatoma longipennis Usinger (Hemiptera, Reduviidae) in peridomestic habitats of a rural community in Jalisco State, Mexico, J. Med. Entomol. 41 (2004) 1015–1020.
- [48] D. Erazo, J. Cordovez, C. Cabrera, J.E. Calzada, A. Saldaña, N.L. Gottdenker, Modelling the influence of host community composition in a sylvatic Trypanosoma cruzi system, Parasitology 144 (2017) 1881–1889.
- [49] H. Abboubakar, J. Claude Kamgang, D. Tieudjo, Backward bifurcation and control in transmission dynamics of arboviral diseases, Math. Biosci. 278 (2016) 100–129